Herpetologica, 80(4), 2024, 358–367

Another New Bent-Toed Gecko of the *Cyrtodactylus marmoratus* Group (Reptilia: Gekkonidae) from West Java, Indonesia

Awal Riyanto[1,3,4], Isna A. Hikmah[2], A.A. Thasun Amarasinghe[1], A. Abinawanto[3], and Amir Hamidy[1]

[1] Research Center for Biosystematics & Evolution, National Research & Innovation Agency (BRIN; Government of Indonesia), Cibinong 16911, Indonesia

[2] Department of Biology, Faculty of Military Mathematics and Natural Sciences, Defense University Republic of Indonesia, Peace and Security Canter (IPSC) Sentul, Bogor 16810, West Java, Indonesia

[3] Department of Biology, Faculty of Mathematics and Natural Sciences, Universitas Indonesia, Kampus UI, Depok, 16424, Indonesia

Abstract: We describe a new species of *Cyrtodactylus* from Sentul, a suburb of Bogor City, West Java, Indonesia that belongs to the *C. marmoratus* species group. The new species is the fourth *Cyrtodactylus* reported from Java. It is small (SVL 46.3–53.8 mm) and nocturnal. A combination of the following characteristics distinguishes the new species from all other congeners: supralabials 11–13; infralabials 9–11; tubercles on the dorsal surface of upper arm absent; tubercles on ventrolateral body folds present; longitudinal dorsal tubercle rows 18–20; paravertebral tubercles 27–34; ventral scale rows 37–40 at midbody; grooved precloacal depression in males; enlarged precloacofemoral scales present, containing 12 or 13 precloacal pores and 2–4 femoral pores; separated by 5–7 normal scales; subdigital lamellae on fourth toe 18–23; and enlarged transverse median subcaudals absent. The new species is genetically divergent from the other two Javan congeners of the *C. marmoratus* group—*C. marmoratus* and *C. semiadii*—with genetic divergences (*p*-distances) of 21.3–22.3% in the mitochondrial ND2 gene.

Key words: Phylogeny; Species complex; Systematics; Taxonomy

Java is one of the biodiversity-rich hotspots on Earth (Cincotta et al. 2000) and it is the thirteenth largest island in the world (Dahl 1991), with an area of ∼128,000 km^2 (Monk et al. 1997). It is almost entirely of volcanic origin and comprises 38 active volcanoes forming an east–west spine (Whitten et al. 1996). This created the island's unique geographical and ecological conditions that have influenced the evolution of Java's gekkonid fauna over millions of years, with many species becoming endemic to the island (O'Connell 2019). So far, only three species of *Cyrtodactylus* are recognized from Java: *C. marmoratus* (Gray 1831), *C. semiadii* Riyanto, Bauer, and Yudha 2014 (Riyanto et al. 2014), and *C. petani* Riyanto, Grismer, and Wood 2015 (Riyanto et al. 2015). *Cyrtodactylus marmoratus* is recognized to be a species complex (see Rösler et al. 2007; Mecke et al. 2016) that includes two nominal species from Java (*C. marmoratus*, *C. semiadii*), a single nominal species from Obi Island (*C. papeda* Riyanto, Faz, and Amarasinghe et al. 2022), and one nominal species from Papua (*C. papuensis* (Brongersma 1934)); the remaining Javanese species, *C. petani*, belongs to the *C. darmandvillei* (Weber 1890) species group, the members of which are mostly distributed in eastern Indonesia to northwestern Australia (Grismer et al. 2021a,b).

Concerning the Javanese members of the *C. marmoratus* group, the distribution of true *C. marmoratus* has been restricted to the wet environs of Cibodas, West Java by Riyanto et al. (2020), whereas *C. semiadii* is distributed in drier parts of central and eastern Java. Based on the phylogenetic studies conducted by Harvey et al. (2015) and O'Connell et al. (2019), it is demonstrated that the cryptic diversity of the *C. marmoratus* group is higher than current understanding. The genetic diversity among Javanese *Cyrtodactylus* encouraged us to conduct comprehensive fieldwork in West Java and a subsequent integrative taxonomic study. Here, we present genetic and morphological data that indicate a series of seven *Cyrtodactylus* specimens from Sentul near Bogor City that represent an additional and previously unrecognized species. Genetic data place these specimens in the *C. marmoratus* group (sensu Grismer et al. 2021a), filling a gap in the wide distribution of this group across Java.

Materials and Methods

In June 2023, we conducted a field training course for undergraduate students from various Indonesian universities at the campus area of the Defense University of Indonesia (Universitas Pertahanan Indonesia, UNHAN) at the Indonesia Peace and Security Center (IPSC), Sentul, a suburb of Bogor City, which has a mountainous topography ranging in elevation from 200–750 m above sea level (Fig. 1). We collected a series of seven *Cyrtodactylus* specimens by hand, euthanized them with sodium pentobarbital, and fixed them in 10% buffered formalin prior to storage in 70% ethanol. We preserved liver tissue samples for DNA analysis in 95% ethanol. Latitude, longitude, and elevation of localities for collected specimens were recorded using a Garmin GPSmap 60CSx using the WGS84 map datum. All specimens are permanently deposited at the Museum Zoologicum Bogorienese (MZB), National Research and Innovation Agency, Cibinong, West Java, Indonesia. Additional comparative material examined for morphological comparisons is listed in the Appendix.

New sequences generated in this work were deposited in GenBank, and additional genetic data were downloaded from GenBank (Supplemental Table S1, available online). As noted above and following Riyanto et al. (2020), we consider DNA sequences from specimens from Cibodas, West Java to represent true *C. marmoratus*. Following Riyanto et al. (2020) and Grismer et al. (2021a), *Gekko gecko* and *Hemidactylus frenatus* were used as outgroups. We extracted genomic DNA from liver samples using a Qiagen DNeasy Extraction Kit. A partial mitochondrial sequence of the protein-encoding gene NADH dehydrogenase subunit 2 (ND2) was amplified with

---

[4] Correspondence: e-mail, awal003@brin.go.id

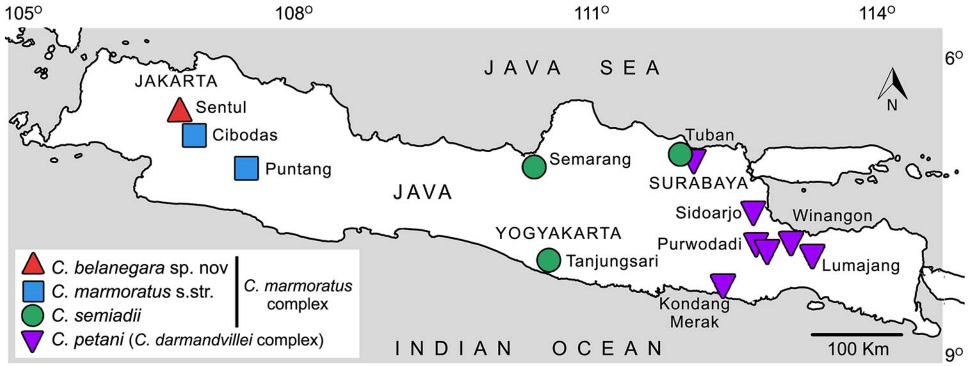

FIG. 1.—Map of Java showing the distribution of the members of *Cyrtodactylus marmoratus* group and *C. petani* (*C. darmandvillei* group) in Java.

the primers M112F (5′-AAGCTTTCGGGGCCCATACC-3′) and M1123R (5′–GCTTAATTAAAGTGTYTGAGTTGC–3′; Oliver et al. 2016). The PCRs were performed in 25 μL total volumes using Top Taq$^{\text{TM}}$ by Qiagen comprising 1.0 μL DNA template, 2.5 μL 10× Top Taq PCR buffer$^{\text{TM}}$, 0.5 μL 10 mM dNTP mix, 2.5 μL 10× CoralLoad, 5 μL 5× Q solution, 1.0 μL light strand primer, 1.0 μL heavy strand primer, 0.125 μL Top Taq DNA polymerase with appropriate buffer and ddH$_2$O to volume. PCR reactions were executed on an Eppendorf Mastercycler under the following conditions: initial denaturation at 94°C for 9 min, second denaturation at 94°C for 45 s, annealing at 60°C for 45 s, and a cycle extension at 72°C for 1 min, for 35 cycles. Purified PCR products were sequenced by 1st Base Asia, Singapore.

We assembled and aligned DNA sequences with available data from GenBank using Clustal W in MEGA X v10.1.7 (Kumar et al. 2018). The uncorrected *p*-distances (sequence divergences) were calculated in MEGA X, and all ambiguous positions were removed for each sequence pair (pairwise deletion option).

We estimated phylogenetic relationships using a final alignment of 1009 base pairs (bp) of the ND2 gene using maximum likelihood (ML) on the IQ-TREE (Nguyen et al. 2015). We used the function -m MFP+MERGE (Lanfear et al. 2012) to identify partitioning strategy and molecular models (first codon TPM2u+F+G4: second codon HKY+F+G4: third codon TPM3u+F+R2). We ran 5,000 bootstrap pseudo-replicates using the ultrafast bootstrap method (UFB; Hoang et al. 2017). Nodes with bootstrap values above 95 were considered highly supported (Minh et al. 2013).

For morphological analyses, we made comparisons with specimens (Appendix) and all the published descriptions of *Cyrtodactylus* from the Great Sunda Islands and Peninsular Malaysia. All specimens examined are held at the MZB. We scored specimens for morphological and morphometric characters used in recent descriptions of the genus *Cyrtodactylus* (e.g., Amarasinghe et al. 2020; Riyanto et al. 2022). Measurements were taken with Mitutoyo digital calipers to the nearest 0.1 mm (except for snout–vent length [SVL] from tip of snout to vent and tail length [TL], which are to the nearest 1 mm) under an AmScope SM-1BZ-RL dissecting microscope on the right side of the body. We took the following measurements: SVL, TL, head length (HL), distance from tip of snout to posterior edge of retroarticular process of lower jaw; head width (HW), in a straight line at angle of jaws; head height (HH), maximum height of head between occiput and throat; snout length (SL), from tip of snout to anteriormost edge of orbit; eye to ear distance (EE), measured from edge of orbit to anterior edge of ear opening; ear length (EL), maximum length of ear opening; orbit diameter (OD), horizontal diameter of orbit; rostral height (RH), maximum height of rostral shield; rostral width (RW), distance between border of rostral shield and first supralabial scales on right and left sides; mental length (ML), maximum length of mental shield; mental width (MW), maximum width of mental shield; forearm length (FAL), taken on dorsal surface posterior margin of elbow while flexed at 90° to inflection of dorsally flexed wrist; axilla–groin length (AG), measured from axilla to groin; and tibia length (TBL), measured on ventral surface from posterior surface of knee while flexed at 90° to base of the heel.

We counted supralabial scales (from the rostral scale to the largest scale immediately posterior to dorsal inflection of posterior portion of upper jaw); infralabial scales (number of labial scales of lower jaw, beginning with first scale bordering mental shield, ending with last enlarged scale bordering angle of jaw); dorsal tubercles rows (number of longitudinal tubercle rows between ventrolateral folds at midbody); paravertebral tubercles (tubercles along paravertebral region, counted between postaxial margin of arm and preaxial margin of leg); ventral scales (number of ventral scales at midbody, counted in one row between ventrolateral folds across the belly); number of lamellae under fingers 1–5 (F_{1-5}, subdigital lamellae counted from point where interdigital skin contacts digit regardless of condition of scales under digit at this point, including fractured scales but not the elongate ungual scale at the base of the claw (claw sheath) or lamellae that extend onto the palm at base of digit); number of lamellae under toes 1–5 (T_{1-5}, subdigital lamellae counted from point where interdigital skin contacts digit regardless of condition of scales under digit at this point, including fractured scales but not including the elongate ungual scale at the base of the claw or lamellae that extend onto plantar surface at the base of the digit). Basal subdigital scales were counted from the most proximal scale at least twice as large as adjacent palmar scales to distalmost lamella at the tip of the digit, following Bauer et al. (2010). In addition, the numbers of precloacal pores, femoral pores, postcloacal tubercles; and separating scales (number of enlarged scales without pores between scales bearing precloacal and femoral pores) were also counted. Where relevant we noted the following characters: presence of tubercles on the dorsal surfaces of the brachium (upper arm), antebrachium (forearm) and

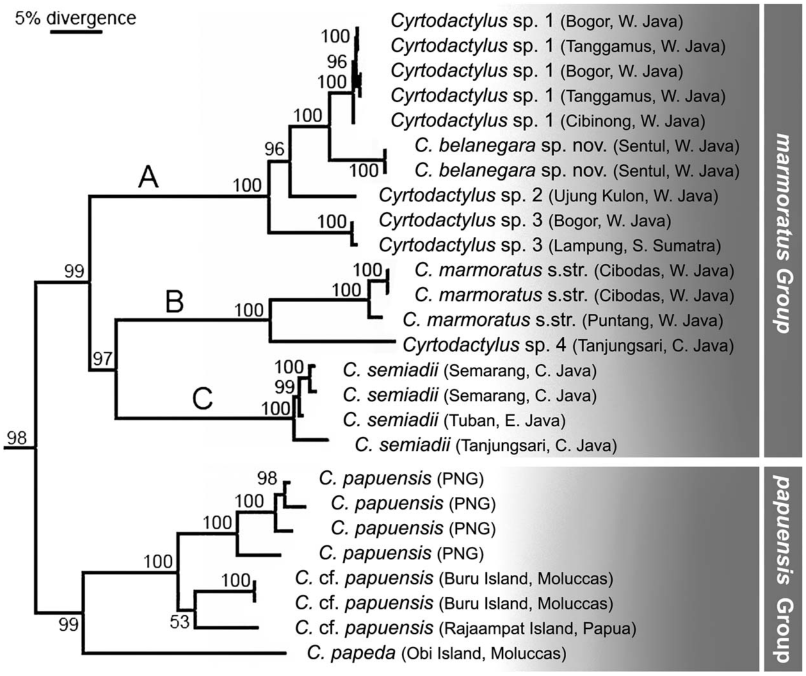

FIG. 2.—The phylogram from ML showing new species within the clade of *Cyrtodactylus marmoratus* group using ~1,009-bp fragment of ND2 mitochondrial gene and its flanking tRNAs.; outgroup taxa, *Gekko gecko* and *Hemidactylus frenatus*, are not shown.

thigh; presence of enlarged precloacofemoral scales, and extent to which these formed a continuous series; and presence of transversely enlarged median subcaudals. We follow Kathriner et al. (2014) and Mecke et al. (2016) in describing the morphology of precloacal depressions. Sex was determined as male if (1) preserved specimens showed enlarged hemipenial pockets, and confirmed by (2) viewing the hemipenes via a small lateral incision made at the base of the tail. In order to examine smaller characters such as keeling on the ventrals, following Amarasinghe et al. (2015) and Harvey et al. (2015), we applied the reversible stain methylene blue in 70% ethanol. Color notes were taken from digital images of living specimens prior to preservation.

To assess the morphometric variation between the new species and its closest congeners from Java, we performed a separate Kruskal–Wallis one-way analysis of variance test because of the small sample size (Zar 2010). A total of 43 adult specimens (19 specimens of *C. marmoratus*, 17 specimens of *C. semiadii*, and 7 specimens of the new species) were used for the statistical analysis. Juveniles were excluded to avoid confounding allometry in the statistical analysis. Statistically informative tests could not be performed on separate sexes because of the smaller sample sizes ($n = 2$) of females representing the new species.

Univariate and multivariate analyses were conducted on seven morphometrics SVL, AG, HL, HW, HH, SL, and OD. Additionally, variation in adult size was normalized using the following equation: $\log X_{\mathrm{adj}} = \log(X) - \beta[\log(\mathrm{SVL}) - \log(\mathrm{SVL}_{\mathrm{mean}})]$, where X_{adj} = adjusted value; X = measured value; β = unstandardized regression coefficient for each population; and $\mathrm{SVL}_{\mathrm{mean}}$ = overall average SVL of all populations (Lleonart et al. 2000; Chan and Grismer 2022). The scaled morphometric data were treated as the dependent variables and the population as the predictor variable. Multivariate analysis was conducted using principal-component analysis (PCA) on the scaled morphometrics above to reduce the highly correlated multidimensional data matrix into a few uncorrelated variables (i.e., principal components [PC]). We used the *princomp* function in the R statistical software program (v4.0.4; R Core Team 2021). Biplots of the first three principal-component scores

TABLE 1.—Uncorrected pairwise sequence divergence (%) for the ND2 protein-coding mitochondrial gene among *Cyrtodactylus marmoratus* group and *C. darmandvillei* group in Java. Sp. 1, 2, 3, and 4 refer to unnamed species.

	Marmoratus group							darmandvillei group
Cyrtodactylus	*C. belanegara* sp. nov	*C. marmoratus*	*C. semiadii*	Sp. 1 (Tanggamus & Bogor)	Sp. 2 (Ujungkulon)	Sp. 3 (Rajabasa & Bogor)	Sp. 4 (Tanjungsari)	*C. petani*
belanegara sp. nov.	—							
marmoratus	21.9	0.0–2.4						
semiadii	21.3–22.3	10.7–21.3	0.09–5.4					
Sp. 1 (Tanggamus & Bogor)	5.0–5.2	22.3–22.8	20.0–21.5	0.0–0.7				
Sp. 2 (Ujungkulon)	10	21.7–22.1	18.4–20.0	10.0–.5	—			
Sp. 3 (Rajabasa and Bogor)	23.0	14.8–15.8	21.0–22.8	23.0–23.6	22.6	—		
Sp. 4 (Tanjungsari)	23.1	14.7–15.7	21.3–23.1	22.0–23.7	22.6	22.0	—	
petani	21.9–22.6	21.5–21.9	18.7–20.2	21.3–22.1	21.7–37.1	23.4–23.6	23.5–23.7	0.0–1.3

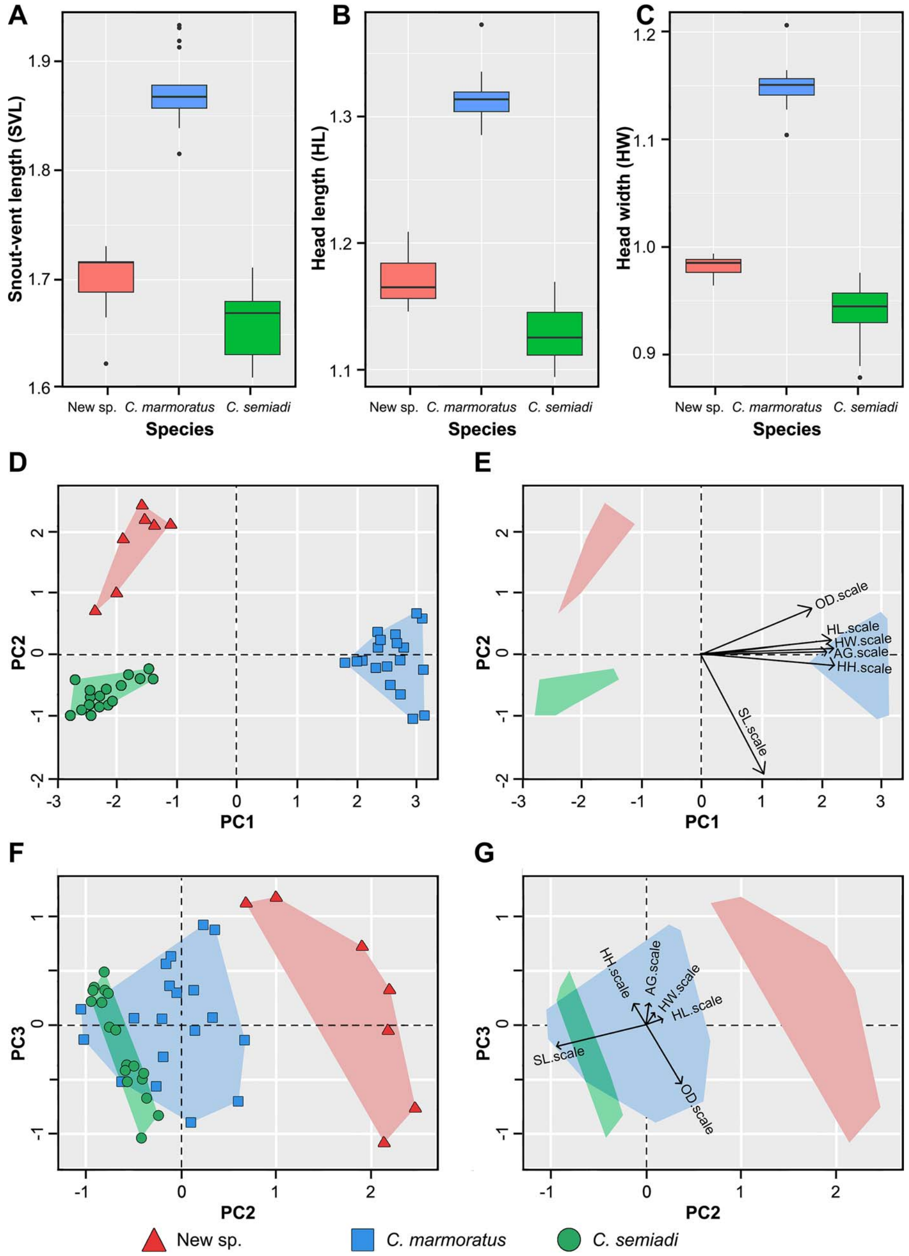

FIG. 3.—Box plots of (A) snout–vent length, (B) head length, and (C) head width indicating differences between the members of *Cyrtodactylus marmoratus* on Java. PCA plots of morphometric variation between the species on Java Island (D, F): *Cyrtodactylus marmoratus* sensu stricto (blue squares), *C. semiadii* (green circles), and the new species (red triangles) clearly shows the morphological distinctiveness of the new species. Each point represents an individual specimen, and the relative distance between two points is equivalent to the amount of dissimilarity. PCA plots with vectors associated with population clusters (E, G).

were used to examine the morphometric differentiation between the species. All statistical analyses were conducted using the R statistical software program (v4.0.4; R Core Team 2021).

RESULTS

Our molecular analysis (Fig. 2), showed that the *Cyrtodactylus* sample from Sentul, Bogor is nested within the *C. marmoratus* group (sensu Grismer et al. 2021a). The *Cyrtodactylus marmoratus* species complex consists of two species groups: the *C. marmoratus* group known from Sumatra (unnamed) and Java and the *C. papuensis* group known from Obi Island and Papua. Within the *C. marmoratus* group, we identified three genetic lineages. Our new species from Sentul is one lineage (Lineage A) with several unnamed species from Bogor, Cibinong, Tanggamus (Sp. 1 sensu Harvey et al. 2015; O'Connell et al. 2019), Ujungkulon (Sp. 2 sensu Grismer et al. 2021a), and Lampung (Sp. 3 sensu Harvey et al. 2015; O'Connell et al. 2019). The *Cyrtodactylus marmoratus* sensu stricto from Cibodas and Gunung Puntang are in one lineage (Lineage B) together with an unnamed species from Tanjungsari (Sp 4). The third lineage (Lineage C) is represented by *C. semiadii* currently known populations from Tanjungsari, Semarang, and Tuban. The genetic divergence (*p*-distance) of samples from Sentul was different from *C. marmoratus* sensu stricto and *C.*

TABLE 2.—PCA and loadings for *C. belanegara* sp. nov., *C. marmoratus*, and *C. semiadii*.

PCA variable	PC1	PC2	PC3	PC4	PC5	PC6	PC7
Standard deviation	2.350	0.9406	0.58672	0.3357	0.27983	0.18219	0.1543
Proportion of variance	0.789	0.1264	0.04918	0.0161	0.01119	0.00474	0.0034
Cumulative percentage	78.9	91.5	96.5	98.1	99.2	99.7	100
Loadings							
Scaled.SVL	0.4075	0.0336	0.2211	0.321	0.8247	−0.0258	−0.0043
Scaled.AG	0.4016	0.0277	0.2555	−0.8696	0.0737	0.1012	0.0270
Scaled.HL	0.4169	0.1022	0.0538	0.0873	−0.2843	−0.7573	−0.3884
Scaled.HW	0.4160	0.0596	0.1303	0.2644	−0.3283	0.6400	−0.4680
Scaled.HH	0.4148	−0.0811	0.1981	0.2409	−0.3449	−0.0101	0.7778
Scaled.SL	0.1975	−0.9195	−0.3231	−0.0337	0.0388	−0.0100	−0.0913
Scaled.OD	0.3386	0.3634	−0.8499	−0.0628	0.0732	0.0753	0.1267

semiadii by a minimum uncorrected *p*-distance of 21.3–22.3%, and to an unnamed species by 5.0–23.1% (Table 1).

All morphometric mean comparisons of the Kruskal–Wallis test also showed significant separation of each species: SVL ($\chi^2 = 32.71$, $P = 7.8^{-8}$), AG ($\chi^2 = 31.68$, $P = 1.3^{-7}$), HL ($\chi^2 = 32.53$, $P = 8.6^{-8}$), HH ($\chi^2 = 31.2$, $P = 1.7^{-7}$), SL ($\chi^2 = 28.2$, $P = 7.4^{-7}$), and OD ($\chi^2 = 20.9$, $P = 2.8^{-5}$), indicating the population of the new species on Java Island has a relatively medium-sized head and body compared to *C. marmoratus* sensu stricto which is larger, and *C. semiadii*, which is smaller. Multivariate analysis by PCA also differentiated the new species population and the closely related *C. semiadii* (Fig. 3A–C). Principal components 1 and 2 collectively explained 91.8% of the variation in the morphometric data matrix (Table 2; Fig. 3D). All the scaled morphometrics were loaded positively with PC 1. Additionally, scaled morphometrics, HH, and SL were loaded negatively with PC 2. Overall, scaled morphometrics SVL, HL, HW, AG, and OD were positively associated with the new species of Java Island (Fig. 3E). Principal components 2 and 3 collectively explained 17.2% of the variation in the morphometric data matrix (Table 2; Fig. 3F). All the scaled morphometrics were loaded positively with PC 2, except for HH and SL. Additionally, scaled morphometrics, SL, and OD were loaded negatively with PC 3. Overall, scaled morphometrics SVL, HL, HW, and AG, were positively associated with the new species of Java Island (Fig. 3G).

SYSTEMATICS

Cyrtodactylus ***belanegara*** *sp.* nov.

(Tables 3, 4; Supplemental Table S2,
available online; Figs. 4A, 5A)

Holotype.—Adult male (MZB.Lace. 15630), from Sentul (6°31.3882′N, 106°53.3613′E, datum = WGS84; 200 m above sea level), Jawa Barat (West Java), Indonesia collected on 24 May 2022 by A. Riyanto and W. Trilaksono.

Paratypes.—Adult males (MZB.Lace. 15631, 15634, 15635, 15636) and adult females (MZB.Lace. 15632, 15633), females, other collection details same as the holotype.

Diagnosis.—The following unique combination of characters distinguishes *C. belanegara* sp. nov. from all other congeners: adults reaching 53.8 mm SVL; supralabials 11–13; infralabials 9–11; tubercles on the dorsal surface of upper arm absent; tubercles on ventrolateral body folds present; longitudinal dorsal tubercle rows 18–20; paravertebral tubercles 27–34; ventral scale rows 37–40; grooved precloacal depression in males; precloacal pores 12–13; femoral pores 2–4, separated from precloacal pores by 5–7 pore less scales; enlarged precloacofemoral scales present; subdigital lamellae on fourth toe 18–23; transversely enlarged median subcaudals absent.

Comparisons.—The new species is most similar to *C. marmoratus* and *C. semiadii*, but differs from *C. marmoratus* in having a smaller body size of 42.0–53.8 mm ($n = 7$) SVL (vs. 69.0–85.21 mm), tubercles on the dorsal surface of lower arms (vs. absent) and discontinuous series of precloacofemoral pores (vs. continuous) in males; from *C. semiadii* in having 12 or 13 precloacal pores (vs. 9–10) in males, 2–4 femoral pores (vs. absent), and a groove-like precloacal depression (vs. absent). The new species also differs from the other *Cyrtodactylus* species in Java, *C. petani*, in having a smaller body size of 53.8 SVL mm (vs. 68 mm), no keeled scales on the dorsal surface of the upper arms (vs. present), tubercles on the dorsal upper arm (vs. absent), and 1 or 2 enlarged precloacofemoral scale rows (vs. 3–4). A detailed comparison of these species is presented in Table 4. We also compare the new species to all recognized Indonesian species for several important characteristics (Supplemental Table S2).

Description of holotype.—Size moderate (SVL = 53.8 mm); head triangular in dorsal view, distinct from neck; tubercles present on the occiput and dorsolateral portion of head; head long, HL = 29.4% of SVL; head rather wide, HW = 66.5% of HL; head wider than high, HH = 50% of HW; snout tapering to relatively blunt tip in dorsal profile, relatively long, OD = 73.0% of SL; loreal region weakly inflated, interorbital region and top of snout concave, canthus rostralis rounded; supraciliaries extending from anteroventral to posterodorsal edge of eye, longest at anterodorsally; ear opening small, dorsoventrally oblong, oriented about 45 degrees to apex of rictus.

Rostral rectangular, RH = 51.4% of RW; bordered posterolaterally by first supralabials and naris, and dorsally by 5 postrostral scales; naris oval, bordered anteriorly by rostral, anterodorsally by 1 postrostral, posteriorly by 3 postnasals on right and 4 on left, and ventrally by first supralabial; orbit separated from supralabials by 2 rows of small lorilabial scales; 13 supralabial scales to angle of the jaw on right, 12 on left; 10 infralabial scales on both sides. Mental triangular, slightly wider than long, ML = 86.9% of MW; bordered laterally by first infralabials, posteriorly by a pair of enlarged first postmentals, in contact medially along 56.3% of length; second postmentals approximately half of first postmentals, separated 5 granular scales; gulars small, granular, decreasing in size posteriorly.

Body elongate, AG = 47.2% of SVL; dorsal scales small, granular, interspersed with large, conical, semiregularly arranged tubercles; ventrolateral body folds with conical tubercles; 19

Table 3.—Meristic and morphometric data of the type series of *C. belanegara* sp. nov., measurements in mm; m = male, f = female, reg = regenerated tail (not measured), NA = not applicable.

	Holotype	Paratypes					
MZBLace	15630	15631	15632	15633	15634	15635	15636
Sex	m	m	f	f	m	m	m
Tuberculation on head	Present	Present	Present	Present	Present	Present	Present
Upper arm tuberculation	Absent	Absent	Absent	Absent	Absent	Absent	Absent
Lower arm tuberculation	Present	Present	Present	Present	Present	Present	Present
Tuberculation on thigh	Present	Present	Present	Present	Present	Present	Present
Tuberculation on tibia	Present	Present	Present	Present	Present	Present	Present
Dorsal scales upper arm	Weakly unikeeled	Weakly unikeeled	Weakly unikeeled	Weakly unikeeled	Weakly unikeeled	Weakly unikeeled	Weakly unikeeled
Precloacal depression	Groove	Groove	Absent	Absent	Groove	Groove	Groove
Postrostrals between nostrils	5	5	5	5	5	5	5
Post mental scales	5	7	5	8	7	7	8
SuL: right(left)	13(12)	13(13)	12(12)	12(11)	12(12)	13(12)	12(12)
InL: right(left)	10(10)	10(11)	10(10)	10(9)	10(10)	11(10)	10(10)
Dorsal tubercles rows	19	19	18	18	18	19	20
Paravertebral tubercles	34	27	28	31	30	32	30
Ventral scales	40	39	40	38	38	37	38
Ventrolateral fold	Tuberculate	Tuberculate	Tuberculate	Tuberculate	Tuberculate	Tuberculate	Tuberculate
Enlarge precloacal scales	Present	Present	Present	Present	Present	Present	Present
Precloacal pores	13	13	NA	NA	13	13	12
Femoral pores: right(left)	4(4)	4(4)	NA	NA	3(3)	2(3)	4(4)
Precloacal and femoral pore separating scales: right(left)	7(7)	6(6)	NA	NA	7(6)	7(6)	6(5)
Post cloacal tubercles	3(3)	2(3)	2(2)	2(2)	2(2)	2(2)	1(1)
T_{1-5}	13-15-17-19-18	12-13-17-20-19	11-17-17-19-16	13-15-16-18-18	9-13-17-23-17	13-16-17-19-18	13-16-16-18-16
SVL	53.8	52.0	52.0	52.1	51.5	46.3	42.0
TL	62.9	reg	reg	reg	reg	reg	48.5
AG/SVL	0.47	0.45	0.42	0.45	0.44	0.44	0.44
TL/SVL	1.17	reg	reg	reg	reg	reg	1.15
HL/SVL	0.29	0.32	0.29	0.31	0.29	0.28	0.30
HW/HL	0.66	0.56	0.68	0.61	0.67	0.69	0.65
HW/HH	2.00	1.58	1.66	1.66	1.68	1.63	1.52
SL/HL	0.42	0.35	0.40	0.38	0.43	0.45	0.37
HH/HL	0.33	0.36	0.41	0.37	0.40	0.42	0.43
OD/HL	0.32	0.23	0.24	0.26	0.22	0.21	0.28
OD/EE	1.45	0.97	0.76	0.75	0.67	0.69	0.94

SuL = supralabials, InL = infralabials, T_{1-5} = lamellae under toes.

TABLE 4.—Selected morphological, morphometric, and meristic characters to diagnose *Cyrtodactylus belanegara* sp. nov. and the Javan species of the *C. marmoratus* group (also including specimens, see Appendix for accession data); NA = not applicable.

	marmoratus group			*darmanvillei* group
	C. belanegara sp.nov.	*C. marmaratus*	*C. semiadii*	*C. petani*
Source	This study	This study	This study	Riyanto et al. (2020)
Maximum SVL	53.8	85.7	51.4	68
Tubercle on head tubercles	Present	Absent	Present	Present
Upper arm tubercles	Absent	Absent	Absent	Absent
Ventrolateral body fold tubercles	Present	Absent	Absent	Indistinct
Abrupt transition	Present	Present	Absent	Present
Precloacal depression	Grooved	Grooved	Wide	Grooved
Enlarged transverse median subcaudal	Absent	Absent	Absent	Absent
Dorsal pattern	Blotched	Blotched	Blotched	Blotched
Dorsal tubercles rows	18–20	11–19	18	15–20
Paravertebral tubercles	27–32	22–29	26–49	25–33
Ventral scales	37–40	34–46	34–45	34–40
Toe 4 lamellae	18–20	17–23	16–20	17–20
Enlarged precloacofemoral scale rows	1, 2	2, 3	Absent	3–4
Enlarged precloacofemoral scales	NA	42–59	Absent	3–40
Precloacal and femoral pore separating scales in males	5–7	NA	NA	NA
Precloacal pores in males	12–13	NA	8–10	NA
Femoral pores in males	2–4	NA	Absent	NA
Precloacofemoral pores in males	NA	24–52	NA	30–40
Post cloacal tubercles	1–3	1–3	1, 2	2, 3

rows of dorsal tubercle; 34 paravertebral tubercles in each row. Ventral scales larger than dorsal scales, smooth, flat, imbricate, 40 ventral scale rows between ventrolateral body folds; enlarged scales immediately anterior to cloacal opening (i.e., pubic patch of enlarged scales).

Forelimbs relatively short, FAL = 14.8% of SVL; dorsal scales on forelimbs weakly unikeeled; tubercles absent on dorsal surface of upper arms; unikeeled tubercles present on dorsal surface of lower arms; palmar scales flat, smooth, subimbricate; digits well developed, inflected at basal interphalangeal joints, digits slightly narrower distal to inflection; subdigital lamellae transversely expanded along the entire length of each digit, but slightly compressed in both length and width immediately distal to interphalangeal inflection; lamellae 13-15-15-14-11; claws well developed, sheathed by 2 dorsal scales and 1 ventral scale.

Hindlimbs longer than forelimbs, TBL = 17.3% of SVL; covered dorsally by granular scales interspersed with larger, conical tubercles; anteroventral scales of thigh rounded, smooth, flat, subimbricate to juxtaposed, larger than dorsal scales; enlarged femoral and precloacal scales arranged in a continuous series, with the enlarged femoral scales arranged in 2 rows; femoral pores and precloacal pores not arranged in a continuous series, separated by 7 poreless scales on each side; femoral pores located at end of enlarged femoral scales, 4 pores on both sides; 13 precloacal pore-bearing scales in groove; posteroventral scales of thigh very small, contrasting with enlarged femoral scales; ventral scales on tibia smooth, flat, subimbricate; plantar scales slightly raised; digits well developed, inflected at basal metapodial–phalangeal joints, digits slightly narrower distal to inflection; subdigital lamellae transversely expanded along entire length of digit, slightly compressed in length and width immediately distal to interphalangeal inflection; lamellae 13-15-17-19-18; claws well developed, sheathed by 2 dorsal scales and 1 ventral scale.

Original tail slightly longer than body, TL = 117% of SVL; segmented, dorsally with keeled tubercles anteriorly 13.0% of its length; three postcloacal tubercles (spur) on each side. Subcaudal scales small, hexagonal, enlarged transverse scales absent.

Coloration.—In life, as in preservative, dorsum dark greenish black; supraciliaries yellowish; iris bright gold with black reticulation; pupil black, bordered light gold; a dark band between nares, above supralabials, and below canthus rostralis to anterior base of the eye, then from a lower base of the eye to nape; a second dark headband forming a semilunar shape, above the first dark band, from the posterodorsal edge of the eye to occiput, where both sides form a Y pattern at the base of the skull; a white band present posterior to the eye; eight paired black blotches crossing between nape and groin; tail with 14 dark bands alternating with 13 white bands, dark bands longer while white bands thin like a ring. Venter pale, except on the subcaudal with 14 dark bands alternating with 13 white bands, the dark bands longer and the white bands thin like a ring.

Variation.—The morphometric and meristic data variation among the type series is presented in Table 3. Female paratypes lack (MZB 15632–3) precloacal and femoral pores but have enlarged precloacal scales. The paratype, MZB 15636 has 12 precloacal pores. The paratype, MZB 15634 has three femoral pores while MZB 15635 has two femoral pores. The precloacal and femoral pore scales were separated by 6six normal scales in MZB 15631 and 15636. Some paratypes (MZB 15632–4 and 15636) have only 12 supralabials. The number of postmental scales (5–8) varies among the paratype series, except for MZB 15632. The number of dorsal tubercle rows varies from 18 (MZB 15632–4) to 20 (MZB 15636). The paravertebral tubercles and ventral scales vary from 27 to 30 and 37 to 40, respectively among the paratype series. All the paratypes have two postcloacal tubercles, except for MZB 15636, which has a single.

Etymology.—The specific epithet is a compound noun in apposition and refers to *belanegara* (in the Indonesian language), composed with the adjective “bela” (=defending) and the noun “negara” (=country). The name refers to the mission of the Indonesia Defense University, where the new species has been found.

Natural history.—Because collections take place during the dry season, we found the new species on dry upstream

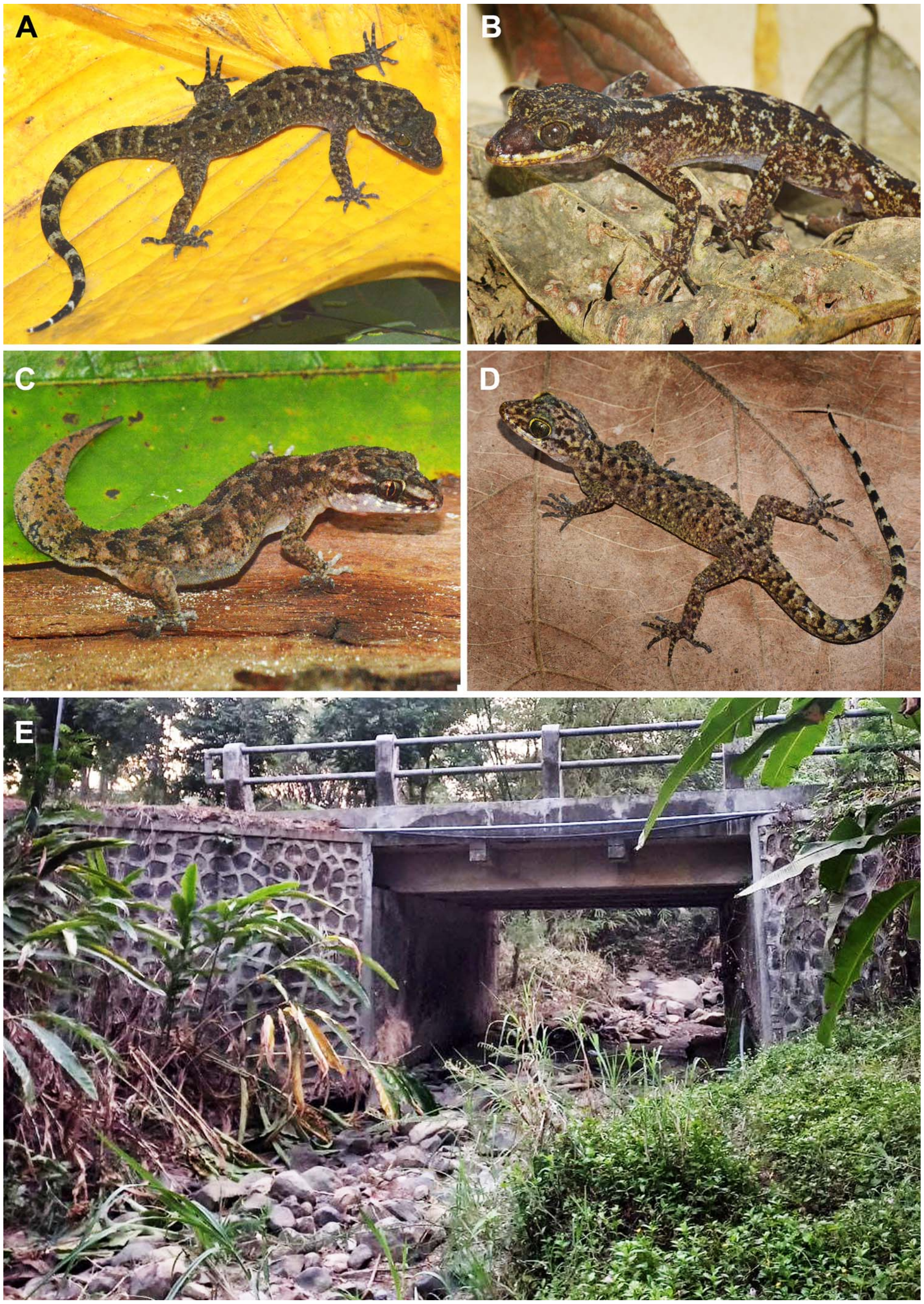

FIG. 4.—The Javanese members of the *C. marmoratus* species group in life: (A) adult male of *Cyrtodactylus belanegara* sp. nov. from Sentul, West Java (holotype, MZB.Lace. 15630), (B) adult male of *C. marmoratus* sensu stricto from Cibodas, (C) adult male of *C. semiadi* from Tuban and the Javanese member of the *C. darmandvillei* species group, (D) adult male of *C. petani* from Tuban, and habitat (E) of *C. belanegara* sp. nov. near a drying stream in Sentul, West Java. Photo by AR and Jusivani.

rock boulders covered with *Adiantum* ferns along the river banks (**Fig. 4E**). The geckos were active when caught, around 2100 h. The first individual was found calling (shrill call: “cek cek cek”) under a man-made bridge.

DISCUSSION

Based on genetic data present in Grismer et al. (2021a) and this study, we consider that the *C. marmoratus* group now includes at least five named species: three from Java (*C. marmoratus*, *C. semiadii*, and *C. belanegara* sp. nov.), one from Melanesia (*C. papuensis*), and one from the Moluccas (*C. papeda*). The linking species between Java and Melanesia are missing, probably because of the lack of sampling in the gap areas. A couple of additional candidate species in this group are known from southern Sumatra (O’Connell et al. 2019). The *C. marmoratus* group is one of three *Cyrtodactylus* lineages that have crossed from the Sunda Shelf into Wallacea and Melanesia, with others being the *C. darmandvillei* group and the ancestor of the main Melanesian radiation of *Cyrtodactylus* (Grismer et al. 2021a,b; Riyanto et al. 2022).

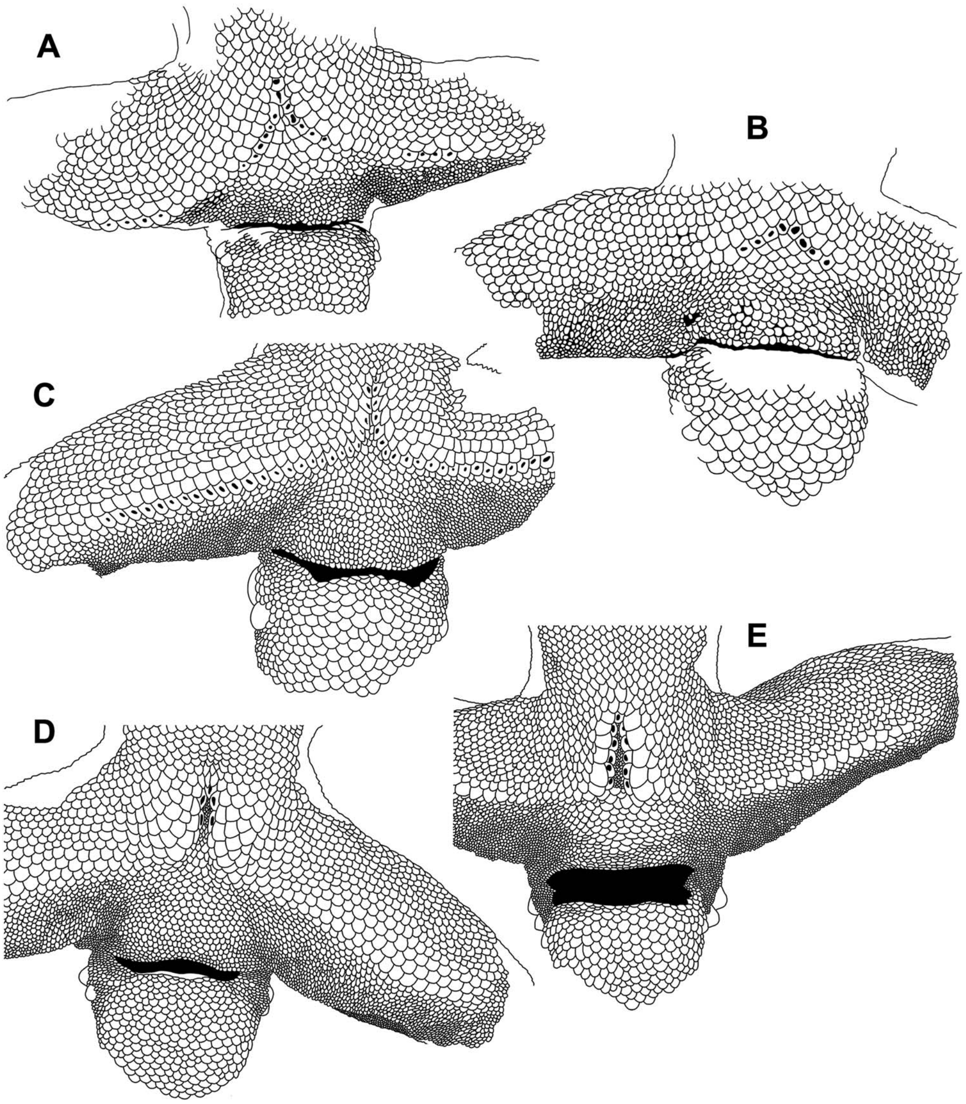

FIG. 5.—Precloacal depression and enlarged femoral and precloacal scales of members of the *C. marmoratus* species group in Indonesia: (A) *Cyrtodactylus belanegara* sp. nov. holotype MZB.Lace. 15630, (B) *C. semiadi* voucher specimen MZB.Lace. 15640, (C) *C. marmoratus* lectotype RMNH.RENA.2710a, (D) *Cyrtodactylus papeda* holotype MZB.Lace. 14052, and (E) *C. papuensis* holotype ZMA.RENA 10937. Illustrations by AR and AATA (not to scale).

Finding new species from the remaining 24% of forests on Java, the most populated island on earth, with over 140 million people (60% of the total population of Indonesia; Ekawati et al. 2015), and which also has undergone massive habitat changes, highlighted the lack of sampling and further strengthened the conclusion that the diversity of Java has not yet been abundantly revealed. Among reptiles, *Cnemaspis muria*—the first existent evidence of the genus *Cnemaspis* on Java—*Cyrtodactylus petani*, and *Cylindrophis subocularis* were discovered from Java during the last decade. Among amphibians, *Polypedates pseudotilophus, Chirixalus trilaksonoi, C. pantaiselatan*, *Leptophryne javanica*, and *Theloderma pseudohorridum* are also new species discovered from Java during the last decade. All these new findings suggest additional unrecognized taxa of herpetofauna await discovery and description in this region.

Acknowledgments.—We thank the Indonesian Institute of Sciences via "KSK–Konstruksi Referensi Sekuen DNA Barcode dan Kajian Genetika Populasi untuk Keperluan Konservasi," CITES, "Forensik dan Pengembangan Bank DNA Fauna Indonesia," and "KSK–Penguatan Kelembagaan dalam Melaksanakan Mandat Sebagai Otoritas Keilmuan Terkait Keanekaragaman Hayati" for support in laboratory work. Other work of this research was funded by the Directorate of Research and Development, Universitas Indonesia under Hibah Puti Q1 2023 (grant NKB-364/UN2.RST/HKP.05.00/2024). AATA thanks E. Dondorp (RMNH, the Netherlands) for sending pictures of specimens under her care. We also thank the staff of the Herpetology Research Group at the National Research and Innovation Agency of Indonesia and acknowledge the support of students in the MBKM program. We thank the Defense University of Indonesia for the permit and facilitating campus surveys.

SUPPLEMENTAL MATERIAL

Supplemental material associated with this article can be found online at https://doi.org/10.1655/Herpetologica-D-24-00023.S1.

LITERATURE CITED

Amarasinghe, A.A.T., M.B. Harvey, A. Riyanto, and E.N. Smith. 2015. A new species of *Cnemaspis* (Reptilia: Gekkonidae) from Sumatra, Indonesia. Herpetologica 71:160–167.

Amarasinghe, A.A.T., A. Riyanto, Mumpuni, and L.L. Grismer. 2020. A new bent-toed species of the genus *Cyrtodactylus* Gray, 1827 (Squamata:

Gekkonidae) from the West Bali National Park, Bali, Indonesia. Taprobornica 9:59–70.

Bauer, A.M., K. Kunya, M. Sumontha, P. Niyomwan, O.S.G. Pauwels, L. Chanhome, and T. Kunya. 2010. *Cyrtodactylus dumnuii* (Squamata: Gekkonidae), a new cave-dwelling gecko from Chiang Mai Province, Thailand. Zootaxa 2570:41–50.

Brongersma, L.D. 1934. Contributions to Indo-Australian herpetology. Zoologische Mededelingen 17:161–251.

Chan, K.O., and L.L. Grismer. 2022. GroupStruct: An R package for allometric size correction. Zootaxa 5124:471–482.

Cincotta, R.P., J. Wisnewski, and R. Engelman 2000. Human populations in the biodiversity hotspots. Nature 404:990–992.

Dahl, A.L. 1991. Island Directory. World Conservation Union (IUCN), Commission on Ecology, Task Force on Conservation of Island Ecosystems in collaboration with the United Nations Environment Programme. UNEP Regional Seas directories and bibliographies. UNEP, Nairobi.

Ekawati, S., K. Budiningsih, Sylviani, E. Suryandari, and I. Hakim. 2015. Kajian Tinjauan Kritis Pengelolaan Hutan di Pulau Jawa. Policy Brief 9:1–8.

Gray, J.E. 1831. A synopsis of the species of Class Reptilia. Pp. 1–110 in The Animal Kingdom Arranged in Conformity with its Organization by the Baron Cuvier with Additional Descriptions of all the Species Hither Named, and of Many Before Noticed (E. Griffith and E. Pidgeon, eds.). Whittaker, Treacher and Co., UK.

Grismer, L.L., P.L. Wood, Jr., N.A. Poyarkov . . . J.L. Grismer. 2021a. Phylogenetic partitioning of the third-largest vertebrate genus in the world, *Cyrtodactylus* Gray, 1827 (Reptilia; Squamata; Gekkonidae) and its relevance to taxonomy and conservation. Vertebrate Zoology 71: 101–154.

Grismer, L.L., P.L. Wood, Jr., N.A. Poyarkov . . . J.L. Grismer. 2021b. Karstic landscapes are foci of species diversity in the world's third-largest vertebrate genus *Cyrtodactylus* Gray, 1827 (Reptilia: Squamata: Gekkonidae). Diversity 13:183.

Harvey, M.B., K.A. O'Connell, G. Barraza, A. Riyanto, N. Kurniawan, and E.N. Smith. 2015. Two new species of *Cyrtodactylus* (Squamata: Gekkonidae) from the Southern Bukit Barisan Range of Sumatra and an estimation of their phylogeny. Zootaxa 4020:495–516.

Hoang, D.T., O. Chernomor, A. Von Haeseler, B. Quang Minh, and L.S. Vinh. 2017. Ufboot2: Improving the ultrafast bootstrap approximation. Molecular Biology and Evolution 35:518–522.

Kathriner, A., A.M. Bauer, M. O'Shea, C. Sanchez, and H. Kaiser. 2014. Hiding in plain sight: A new species of bent-toed gecko (Squamata: Gekkonidae: *Cyrtodactylus*) from West Timor, collected by Malcolm Smith in 1924. Zootaxa 3900:555–568.

Kumar, S., G. Stecher, M. Li, C. Knyaz, and K. Tamura. 2018. MEGA X: Molecular evolutionary genetics analysis across computing platforms. Molecular Biology and Evolution 35:1547–1549.

Lanfear, R., B. Calcott, S.Y.W. Ho, and S. Guindon. 2012. Partitionfinder: Combined selection of partitioning schemes and substitution models for phylogenetic analyses. Molecular Biology and Evolution 29:16951701.

Lleonart, J., J. Salat, and G.J. Torres. 2000. Removing allometric effects of body size in morphological analysis. Journal of Theoretical Biology 205:85–93.

Mecke, S., M. Kieckbusch, L. Hartmann, and H. Kaiser. 2016. Historical considerations and comments on the type series of *Cyrtodactylus marmoratus* Gray, 1831, with an updated comparative table for the bent-toed geckos of the Sunda Islands and Sulawesi. Zootaxa 4175:353–365.

Minh, B.Q., M.A.T. Nguyen, and A. von Haeseler. 2013. Ultrafast approximation for phylogenetic bootstrap. Molecular Biology and Evolution 30:1188–1195.

Monk, K.A., de Y. Fretes, and G.R. Liley. 1997. The Ecology of Nusa Tenggara and Maluku, Volume V. Periplus editions, Singapore.

Nguyen, L.T., H.A. Schmidt, A. von Haeseler, and B.Q. Minh. 2015. IQ-TREE: A fast and effective stochastic algorithm for estimating maximum likelihood phylogenies. Molecular Biology and Evolution 32:268–274.

O'Connell, K.A., U. Smart, I. Sidik, A. Riyanto, N. Kurniawan, and E.N. Smith. 2019. Diversification of bent-toed geckos (*Cyrtodactylus*) on Sumatra and west Java. Molecular Phylogenetics and Evolution 134:1–11.

Oliver, P.M., S.J. Richards, Mumpuni, and H. Rösler. 2016. The Knight and the King: Two new species of giant bent-toed gecko (*Cyrtodactylus*, Gekkonidae, Squamata) from northern New Guinea, with comments on endemism in the North Papuan Mountains. ZooKeys 562:105–130.

R Core Team. 2021. R: A Language and Environment for Statistical Computing, Version 4.0.4. Available at https://www.R-project.org/. R Foundation for Statistical Computing, Austria. Accessed on 25 February 2021.

Riyanto, A., A.M. Bauer, and D.N. Yudha. 2014. A new small karst-dwelling species of *Cyrtodactylus* (Reptilia: Squamata: Gekkonidae) from Java, Indonesia. Zootaxa 3785:589–599.

Riyanto, A., A. Farajallah, A. Hamidy, Y.S. Fitriana, M. Munir, N. Kurniawan, and E.N. Smith. 2020. Taxonomic evaluation of two similar bent-toed geckos (Squamata: Gekkonidae: *Cyrtodactylus* Gray, 1827) from East Java, Indonesia. Zootaxa 4830:186–196.

Riyanto, A., F.H. Faz, A.A.T. Amarasinghe, M. Munir, Y.S. Fitriana, A. Hamidy, M.D. Kusrini, and P.M. Oliver. 2022. New bent-toed gecko of the *Cyrtodactylus marmoratus* group (Reptilia: Gekkonidae) from Obi Island, Indonesia. Herpetologica 78:30–39.

Riyanto, A., L.L. Grismer, and P.L. Wood, Jr. 2015. *Cyrtodactylus rosichonariefi* sp. nov. (Squamata: Gekkonidae), a new swamp-dwelling bent-toed gecko from Bunguran Island (Great Natuna), Indonesia. Zootaxa 3964:114–124.

Rösler, H., S.J. Richards, and R. Günther. 2007. Remarks on morphology and taxonomy of geckos of the genus *Cyrtodactylus* Gray, 1827, occurring east of Wallacea, with descriptions of two new species (Reptilia: Sauria: Gekkonidae). Salamandara 43:193–230.

Weber, M. 1890. Reptilia from the Malay Archipelago. 1. Sauria, Crocodylidae, Chelonia. Pp. 158–177 in Zoologische Ergebnisse einer Reise in Niederländisch Ost-Indien 1 (M. Weber, ed.). E.J. Brill, The Netherlands.

Whitten, A.J., R.E. Soeriaatmadja, and S.A. Afiff 1996. The Ecology of Java and Bali, vol. 2. Periplus Editions, Singapore.

Zar, J.H. 2010. Biostatistical Analysis, 5th edition. Prentice Hall, USA.

Accepted on 16 July 2024
ZooBank.org registration LSID: 0CD3C709-D587-423C-AA34-EF2ED668C480
Published on 8 October 2024
Associate Editor: Christopher Raxworthy

APPENDIX

Other Specimens Examined

Cyrtodactylus batik.—Indonesia: Central Sulawesi: MZB.Lace. 8511 (holotype).

Cyrtodactylus celatus.—Indonesia: Timor: TBMNH 1926.10.30.45 (holotype), ZSM 556/2002.

Cyrtodactylus darmandvillei.—Indonesia: Flores: ZMA.RENA 10943–44 (syntypes); Timor: FMNH 154845.

Cyrtodactylus deveti.—Indonesia: Halmahera: MZB.Lace. 7956, 8164–65; Morotai Island: RMNH 2775 (holotype), 8683 (paratype).

Cyrtodactylus fumosus.—Indonesia: North Sulawesi: NMB 2662 (holotype).

Cyrtodactylus gordongekkoi.—Indonesia: Lombok: ZRC 2.3381 (paratype).

Cyrtodactylus halmahericus.—Indonesia: Halmahera: MZB.Lace. 6087, 13250.

Cyrtodactylus hitchi.—Indonesia: Southeast Sulawesi: MZB.Lace. 8642 (holotype), 8635–40 (paratypes), 8646 (paratype), 8648 (paratype).

Cyrtodactylus jatnai.—Indonesia: Bali: UIMZ 0085 (holotype), UIMZ 0082–84 (paratypes), 0101–102 (paratypes), MZB.Lace. 8725–37 (paratypes).

Cyrtodactylus jellesmae.—Indonesia: Central Sulawesi: NMB 2660 (lectotype); South Sulawesi: MZB.Lace. 5686, 5688; North Sulawesi: NMB 2661 (paralectotype); MZB.Lace. 6943.

Cyrtodactylus laevigatus.—Indonesia: Komodo: MZB.Lace. 979.

Cyrtodactylus marmoratus.—Indonesia: Cibodas, West Java: MZB.Lace.9706–11, 12123–24, 15686.

Cyrtodactylus nuaulu.—Indonesia: Seram: MZB.Lace. 2326 (holotype), 2325, 2327–28, UIMZ 0181.

Cyrtodactylus papuensis.—Southern New Guinea: ZMA.RENA 10937 (holotype); Indonesia: West Papua: MZB.Lace. 12115, 14969–70, 15160–66.

Cyrtodactylus semiadi.—Indonesia: Central Java: MZB.Lace. 15670–75, 15681–82; East Java: MZB. Lace. 15676–80; Yogyakarta: MZB. Lace. 15683–85.

Cyrtodactylus spinosus.—Indonesia: Central Sulawesi: MZB.Lace. 7024 (holotype), 7025–29 (paratypes).

Cyrtodactylus tahuna.—Indonesia: Sangihe Island, North Sulawesi: MZB.Lace. 5123 (holotype), 5097, 5133 (paratypes).

Cyrtodactylus tambora.—Indonesia: Sumbawa: MZB.Lace. 3298 (holotype), 13297, 13909 (holotypes).

Cyrtodactylus tanahjampea.—Indonesia: Tanahjampea Island, South Sulawesi: MZB.Lace. 5675 (holotype), 5671–72 (paratypes), 5674 (paratype).

Cyrtodactylus wallacei.—Indonesia: Kabaena Island, Southeast Sulawesi: MZB.Lace. 4264 (paratype).

Cyrtodactylus zugi.—Indonesia: Raja Ampat Archipelago (West Papua): MZB.Lace. 5574 (holotype), 5573 (paratype), 5575 (paratype).